Proceedings World Geothermal Congress 2015
Melbourne, Australia, 19-25 April 2015

3-D Seismic Velocity and Attenuation in the Central Taupo Volcanic Zone, New Zealand: Imaging the Roots of Geothermal Systems

Stephen Bannister[1], Sandra Bourguignon[1], Steve Sherburn[2] and Ted Bertrand[1]

[1]GNS Science, Avalon 5010, New Zealand

[2]GNS Science, Wairakei, Private Bag 2000 Taupo 3352

s.bannister@gns.cri.nz

Keywords: Seismicity, Taupo Volcanic Zone, Seismic velocity, Seismic attenuation

ABSTRACT

We image the crustal seismic properties beneath a 30 x 50 km area of the Taupo Volcanic Zone (TVZ), New Zealand, encompassing the Wairakei, Mokai, Rotokawa, Ngatamariki, and Ohaaki geothermal fields, as part of a multi-disciplinary research program to investigate the untapped deep geothermal resource in this region. The focus of the study is to resolve seismic properties in the 2-8 km depth range. Our study of seismic properties is complementary to a magnetotelluric study investigating electrical conductivity in the same region (Bertrand et al., 2012a; 2012b; 2013). Seismic data used for the imaging was recorded using a 38-site broadband seismic array deployed across the region between September 2009 and April 2011 with an average station spacing of ~4-7 km. We supplement this new broadband data with legacy short-period and broadband data recorded by previous research seismic arrays, including the 1995 "TVZ95" array, the 2001 "CNIPSE" array, the "RF2004" array, data recorded by the national GeoNet seismometer network, and with active source data collected in the "NIGHT" experiment in 2001. The combined dataset is comprised of 1347 well-recorded earthquakes and 9 explosions, recorded at 925 recording stations, providing more than 120,200 differential travel time measurements, calculated using the absolute times from pairs of neighbouring earthquakes. We invert these data to derive the spatial and depth variation of seismic properties Vp, Vs, Vp/Vs, and Q (1/attenuation), beneath the area encompassing the geothermal field. The final 3-D Vp, Vp/Vs, Qp and Qs volumes show a high level of heterogeneity at a range of length scales, especially for Q, illustrating that older simplified 2-D models are inappropriate for the region.

1. INTRODUCTION

The Taupo Volcanic Zone (TVZ) is an actively rifting continental arc (Wilson et al.,1995) that is related to subduction of the Pacific Plate beneath the North Island of New Zealand, along the Hikurangi margin. The central part of the TVZ, north of Lake Taupo (Figure 1), is marked by extensive rhyolitic volcanism and includes 23 high-temperature geothermal systems. Development of 'conventional' geothermal energy, from depths of 1-3 km where reservoir temperatures reach 330°C contributes ~13% (~800 MWe) of New Zealand's electricity supply. However, estimates of the deep geothermal resources at depths of up to 5-7 km (where temperatures are likely to exceed 400°C) could exceed 10,000 MWe (Bignall, 2010).

To better understand New Zealand's deep geothermal resource potential, a multi-institutional research programme was established in 2008 to investigate links between the shallow hydrothermal systems and the deeper magmatic heat source that is thought to drive convection within the brittle crust. This research included the collection of magnetotelluric (MT) and passive-seismic measurements in central TVZ, north of Lake Taupo (Figure 1). These complementary MT and passive-seismic surveys were designed to identify structure within the basement rocks at depths between 3 and 8 km, to help advance our understanding of the process that transport heat to the surface. Research to date has included very intensive magnetotelluric observations and 3D inversion for electrical properties of the mid-crust (Bertrand *et al.*, 2012a; 2012b; 2013; Heise *et al.*, 2010) and initial seismological investigation (Bannister *et al.*, 2013).

The new passive-seismic broadband data were recorded for this deep-geothermal research programme using a dense 38-site broadband seismic array, which was deployed across the region between September 2009 and April 2011. The seismic array had an average station spacing of ~4-6 km (Figure 1). We supplement this new broadband data with legacy short-period and broadband data recorded by previous research seismic arrays from 1995 onwards, including the 1995 "TVZ95" array (Bryan *et al.*, 1999; Sherburn *et al.*, 2003) , the 2001 "CNIPSE" array (Reyners *et al.*, 2006), the "RF2004" broadband array data collected in 2004, short-period and broadband data recorded by the New Zealand national GeoNet seismometer network (Petersen et al., 2011), and active-(explosion) source data collected in the "NIGHT" experiment in 2001 (Harrison and White, 2006; Henrys *et al.*, 2003) (Figure 1). The combined dataset is comprised of 1198 well-recorded earthquakes (Figure 3) and 9 explosions, recorded at 925 recording stations.

Using the new seismic data we focus here on resolving higher-order variation of bulk seismic properties of the crust, in the same region as already covered by the magnetotelluric observations, focusing especially on the 3-to-8 km depth range. Initial seismic analysis is described in Bannister *et al.* (2013). The seismic properties we target include P-wave velocity (Vp) and the S-wave velocity (Vs). We also use the seismic waveform characteristics to determine the 3D variation of seismic attenuation (1/Qp and 1/Qs), which is an excellent indicator of temperature.

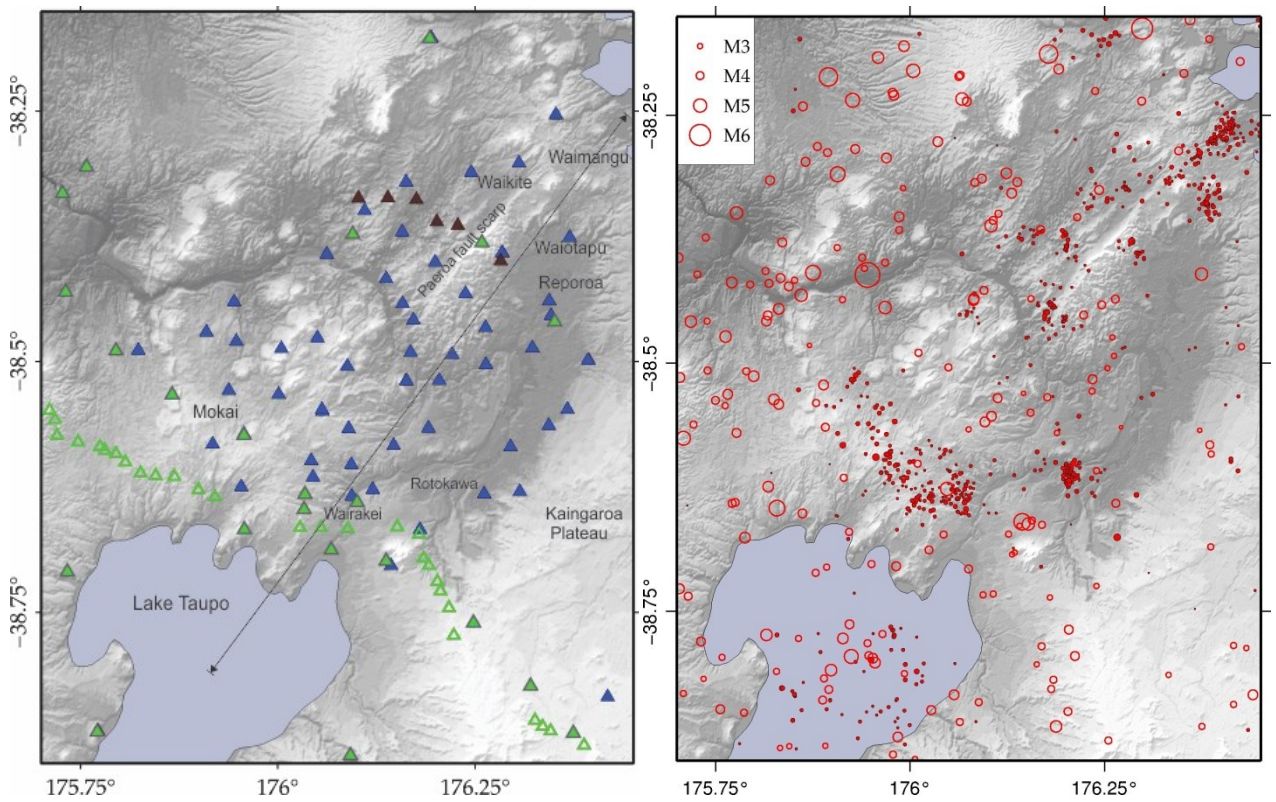

Figure 1a: (Left) Distribution of seismometers deployed in the Taupo Volcanic Zone, for which seismic data were available for this study. Solid line is the location of the profile used in cross-sections for Figures 3-5. Station symbols are CNIPSE: green solid triangles; Harrison & White (2006) array: green open-triangles; HD2009-2011 array: blue triangles ; RF2004 array: dark red triangles. Figure 1b (Right) Distribution of the 1198 earthquakes used in the seismic tomography inversion. Solid red circles represent events shallower than 40 km; open red circles are earthquakes deeper than 40 km. The symbol size scales with the earthquake magnitude.

2. INVERSION FOR VELOCITY STRUCTURE

2.1 Approach

P-phase and S-phase arrival times were picked for all of the earthquakes recorded by the 2009-2011 broadband seismic array, and arrival-pick uncertainties were then automatically assigned on the basis of the signal-to-noise ratio. P-arrival times were picked on vertical component data, and S-wave arrivals were picked on horizontal component data, where available, out to stations more than 120 km offset from the epicenter. Previous seismic data and seismic arrival time phase picks from previous seismic experiments were re-examined manually before incorporating into the full combined dataset. Additional S-phase arrival times were picked for many of the legacy datasets.

These arrival times were then used to retrieve a 3D velocity model for the region, to examine the velocity heterogeneity beneath the region, and to allow much improved earthquake location. To derive these new estimates of 3D seismic velocity we apply the double-difference (DD) tomography method of Zhang and Thurber (2003), jointly inverting for earthquake hypocentres, and seismic parameters P-wave velocity (Vp), S-wave velocity (Vs) and Vp/Vs. The technique of Zhang and Thurber minimizes residuals between observed and calculated arrival-time differences for pairs of closely located earthquakes, while also minimizing the residuals of absolute arrival times. Their approach builds on the location procedure of Waldhauser and Ellsworth (2000), which utilises the differential times of P and S phase times. In addition to solving for the hypocentre parameters, the algorithm solves for the 3-D velocity structure in the model region, requiring additional smoothing parameters, as described by Zhang and Thurber (2003).

In the analysis for this study we only utilise catalogue differential times, which are derived from the phase pick arrival times of the P and S phases. The available earthquakes and recordings in the combined dataset provide more than 120,000 differential travel time measurements, which were calculated using the absolute times from pairs of neighbouring earthquakes. Initial hypocenter locations for the double-difference inversion were determined by New Zealand GeoNet (http://www.geonet.org.nz), for events detected and located by GeoNet. The full range of earthquakes in the combined inversion dataset comprises an excellent range of shallow crustal earthquakes, as well as deeper background seismicity, comprised of larger earthquakes occurring in the subducted Pacific plate, which lies at greater than 50 km depth beneath the TVZ. The information contained in the arrival-times from the deeper subduction earthquakes (which range between 40 and 200 km depth) helps to constrain the deeper crustal structure, while the shallower earthquakes provide the detailed information for refining the shallow crustal structure. The final data set provides the best possible coverage of the Taupo Volcanic Zone shallow crustal structure to date, of any seismic data set, and samples beneath many of the geothermal fields currently tapped for geothermal power. New additional GeoNet stations are installed in the region each year. In the future we will use data from any additional stations to further improve the seismic wave path coverage through the upper-mid crust, and further improve the resolution of the seismic property volumes derived from that data.

Catalogue-based differential times (CTDT) were calculated between closely spaced events from manually picked P- and S- phase times. Differential times were calculated for event pairs initially separated by less than 10 km, for all stations less than 140 km from the particular cluster centroid. Use of such a maximum separation criteria reduces the total number of required correlation calculations, but is justifiable, as the correlation between different events typically decreases rapidly with increasing inter-event separation, and the assumptions underlying the use of differential times also becomes poor with increasing event separation (Waldhauser, 2001; Waldhauser & Ellsworth, 2000). Once calculated, the CTDT differential times were then combined with the absolute arrival times (arrival times of picked P and S phases) and simultaneously inverted using the double-difference-tomography algorithm of Zhang and Thurber (2003), in an iterative least-squares procedure which utilises the LSQR method (Paige and Saunders, 1982). The full dataset was comprised of 25820 absolute P-times, 13596 absolute S phases, 13141 absolute S-P times, and 128559 differential times.

Travel-time calculations were initially carried out using a velocity model based on the current New Zealand 3D velocity model, previously derived by Eberhart-Phillips *et al.*, (2010) from earthquake data. This 3D New Zealand model is reasonably well defined in the Taupo Volcanic Zone, down to more than 300 km depth, primarily due to some intensive tomography work carried out in 2001-2006 (Eberhart-Phillips *et al.*, 2010; Reyners *et al.*, 2006), in which passive-source seismic data from the North Island CNIPSE experiment (Reyners *et al*., 2006) was used to constrain the model.

We gradationally interpolated the existing 3D New Zealand model velocities onto a much finer grid to encompass our study region, and to focus on the depth range of interest. Our final finest-level inversion grid has a minimum grid spacing of 7.5 km along the x- and y-axes, in the section of the inversion volume with the highest ray path coverage, and grid layers at 1, 2.5, 4, 5.5, 7, 9, 11, 14, 18, 23, 30, 34, and 38 km depth, in the top 40 kms, fully encompassing the range of depths of interest (Figure 2). Deeper inversion nodes were retained from the New Zealand 3D wide velocity grid, down to depths of 367 km. Our inversion strategy involved slowly increasing the inversion node density, starting with the New Zealand wide 3D velocity grid, and slowly increasing the node density between inversions, to the grid density described above. This gradational approach to the velocity inversion has been recognised in other studies to provide stable results, especially critical for heterogeneous regions such as the TVZ.

The 3D P-wave velocity (Vp), shear-wave velocity (Vs) and the Vp/Vs ratio were derived as part of the tomographic inversion. In addition the 1198 earthquakes used in the inversion were relocated using the final 3D Vp and Vp/Vs solution models and the P and S cross-correlation times optional to the double-difference method (Waldhauser, 2001).

2.2 Derived velocity estimates

Figure 2 shows depth slices of the resulting P-wave velocity (Vp) volume after inversion, sliced horizontally at 4 and 6 km depth below sea level. We use the derivative weight sum (DWS) (Thurber, 1993; Thurber and Eberhart-Phillips, 1999) at each grid node as a measure of the seismic path coverage and resolution; nodes with low DWS (indicating poorer path coverage) are masked in the figures shown below. The velocity structure is well resolved in the centre of the study region (i.e. inside the bounds of the 2009-2011 seismometer array), although not to the east, on the Kaingaroa Plateau, nor to the north-west, due to the sparsity of recording seismometer stations outside of the TVZ, and the lower level of seismic activity at crustal depths for those areas.

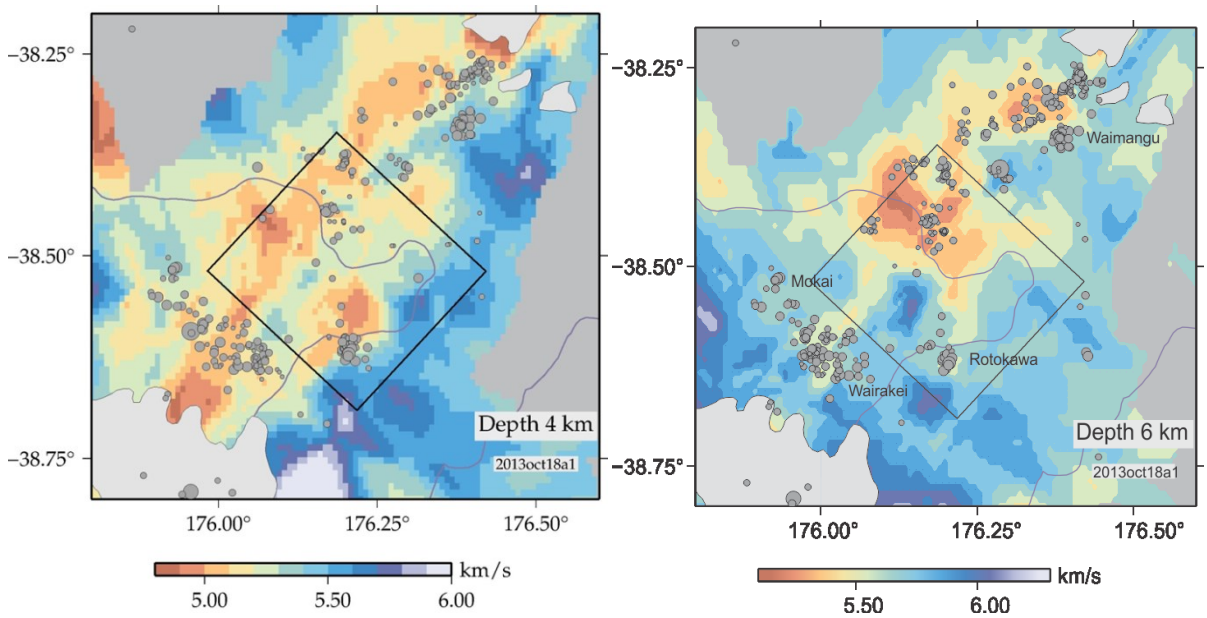

Figure 2: P-wave velocity (km/s) at (left) 4 km depth and (right) 6 km depth, slicing through the new revised 3D P-wave velocity volume derived from seismic tomography. Earthquakes within +/- 1 km of each depth slice are projected onto the slice. Areas that are not well constrained have a grey mask applied, based on the P-wave Derivative Weight Sum. The marked square outlines the spatial area covered by a complementary densely spaced magnetotelluric (MT) survey, which is described by Bertrand et al. (2012a).

At 4 kms depth we note seismic activity (projected from 4 +/- 1 km) associated with west Wairakei geothermal field and Rotokawa geothermal field, as well as north of Waiotapu, while at 6 (+/- 1 km) depth there is seismicity north-west of Waimungu, and also

near Mokai geothermal field. Further relocation analysis using waveform-based differential travel times (e.g. Waldhauser, 2001, Waldhauser and Ellsworth 2000, Zhang and Thurber, 2006) is necessary to confirm the depth of the seismic-aseismic transition, and whether there are substantial spatial changes in the transition depth beneath the region, and beneath individual geothermal fields. Any such changes that we determine are expected to closely relate to spatial changes in the temperature. Low Vp, less than 5 km/s, is observed at 4 km depth in the area north-west of Waikite, and also along the north edge of Lake Taupo. At 6 km depth (Figure 2) Vp varies between ca. 5.3 km/s and 6 km/s, with lower Vp values west of the Paeroa fault scarp.

Figure 3 shows a SW-NE-oriented cross-section of the derived Vp, slicing through the new P-wave velocity volumes at a strike of N120E. The cross-section of Vp shows a moderate level of 3D heterogeneity, especially at ca. 5-15 kms depth, while there are also large-scale (> 20% variability over 20 km distance) changes in Vp at 10-30 kms depth. At the shorter scale, other slices of the Vp volume (not shown) suggest small, thin, higher Vp bodies at between 5 and 7 km depth. These may possibly represent solidified plutonic material (e.g. Wilson et al., 2006). The scale of these bodies appears to be around 5 km, which is at the resolution limit of our data inversion. Further resolution testing and synthetic modelling needs to be carried out to confirm the details of the bodies. It is clear from the highly spatially-variable Vp that previous simplistic 2-D interpretations of TVZ crustal structure are not appropriate in this region.

Figure 4 shows the ratio Vp/Vs along the same SW-NE-oriented cross-section. P-wave and S-wave arrivals are both necessary to derive Vp/Vs, so the path coverage in the Vp/Vs volume is lower than for just the P-wave velocity (Vp) volume. Areas on the cross-section shown in Figure 4 which are not well sampled are masked (in light grey), based on the derivative-weight-sum (DWS) values calculated in the inversion. Moderately high Vp/Vs values are observed in the near-surface, beneath Wairakei geothermal field, at X=20-30 km. A low Vp/Vs feature at 5-7 km depth is consistently observed on different cross-sections through the Vp/Vs volume, observed at X=40-50 km on Figure 4. At this stage we interpret this low Vp/Vs feature as representing Torlesse basement Terrane, which in surface exposures is dominated by quartz-rich turbidites (Adams et al., 2009). The composition of the basement terrane is inferred to change markedly beneath the region, becoming increasingly felsic to the west (Adams et al., 2009).

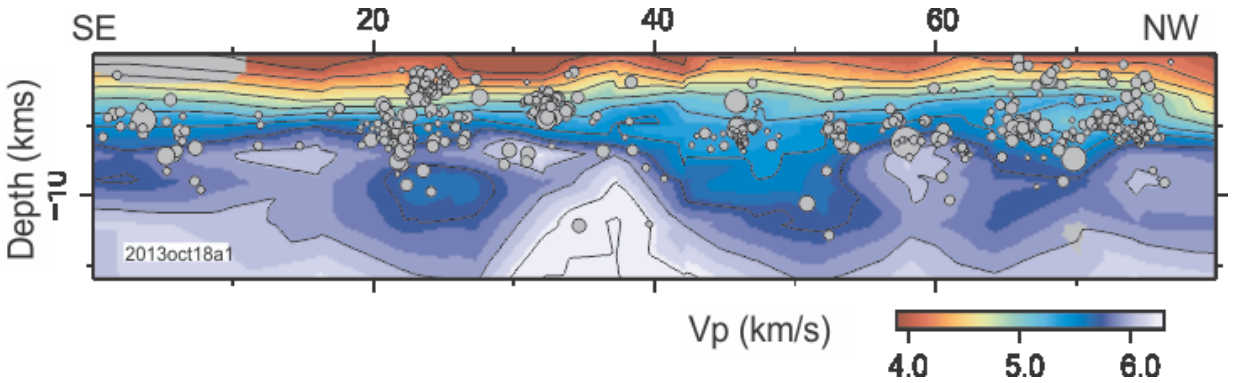

Figure 3: A SE-NW cross-section of Vp (km/s) along the profile shown in Figure 1a. Wairakei seismicity is projected onto this cross-section at X=20-25 km, and Waiotapu-Waimangu seismicity at X=65-75 km.

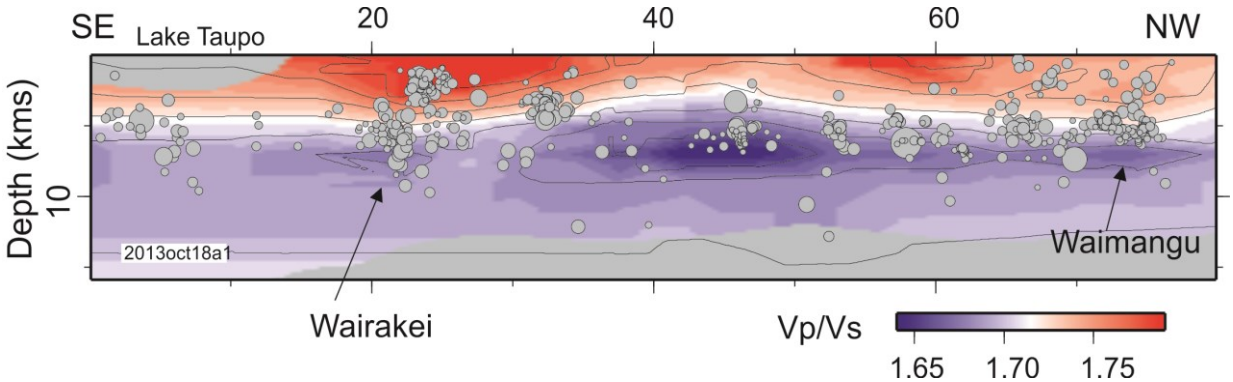

Figure 4: A SE-NW cross-section of the ratio Vp/Vs along the profile shown in Figure 1a. Areas that are not well constrained are masked, based on the derivative-weight-sum (DWS).

3. INVERSION FOR ATTENUATION STRUCTURE

3.1 Approach for inversion for Q

Using the broadband seismic waveforms recorded on the 2009-2011 seismic array we also examine the attenuation between earthquakes and seismometers, and derive 3-D volumes of the dimensionless quality factor Q (1/attenuation) using those observations. High Q represents low attenuation, and low Q represents high attenuation. Attenuation studies have been carried out throughout New Zealand, but previously at a larger crustal-mantle scale (e.g. Eberhart-Phillips *et al.*, 2008, 2014). In this study we focus on estimating Q just for the 0-10 km depth range.

We analyse the velocity amplitude spectra from our best quality waveform data, to determine t* values for both P waves and S waves (e.g. Eberhart-Phillips *et al.*, 2014). We then invert those t* values for 3-D frequency-independent Qp and Qs models of the crustal attenuation, following the approach of Bennington *et al.* (2008) for the inversion, allowing for site-specific terms. In further planned work we will be examining the frequency dependence of our results in detail, which we expect to be important given the temperature dependence of Q. The results shown below are assuming that Q is frequency independent in the frequency range ca.1-20 Hz.

3.2 Derived attenuation volume

Figure 5 shows SE-NW cross-sections of the Qp and Qs structure, along the same profile as for Figures 3 and 4. These cross-sections show a prominent high-Q feature (with Q > 250) at between 5 and 10 km depth. The high-Q feature is not continuous along the full profile, with a distinct break beneath the Wairakei geothermal field. Attenuation increases with increased porosity or crack density, with a linear relationship between 1/Q and crack density (Peacock *et al.*1994). Q can also be affected by impedance contrasts, chemical composition, fluid saturation and, importantly in this region, temperature variations (e.g. Fontaine *et al.*2005). Such dependencies make the interpretation of Q quite challenging. Full detailed interpretation of these results requires the use of cross-parameter examination, (e.g. examining the multi-correlation between the seismic properties Vp, Vs, and Vp/Vs, Qp, Qs, as well as the resistivity volume derived from the 3-D MT research), which we intend to carry out following approaches similar to that described by Zhang *et al.*(2009) and Bedrosian *et al.*(2007). At this stage one interpretation of the high-Q feature would involve it representing a spatially-discontinuous Torlesse basement terrane. At greater depth there are low-Q features apparent in both Qp and Qs, at depths greater than 8-10 km (e.g. at X=65-70 km in Figure 5); we continue to test the robustness of these features in inversion tests, and their correspondence with high conductivity bodies highlighted from magnetotelluric observations.

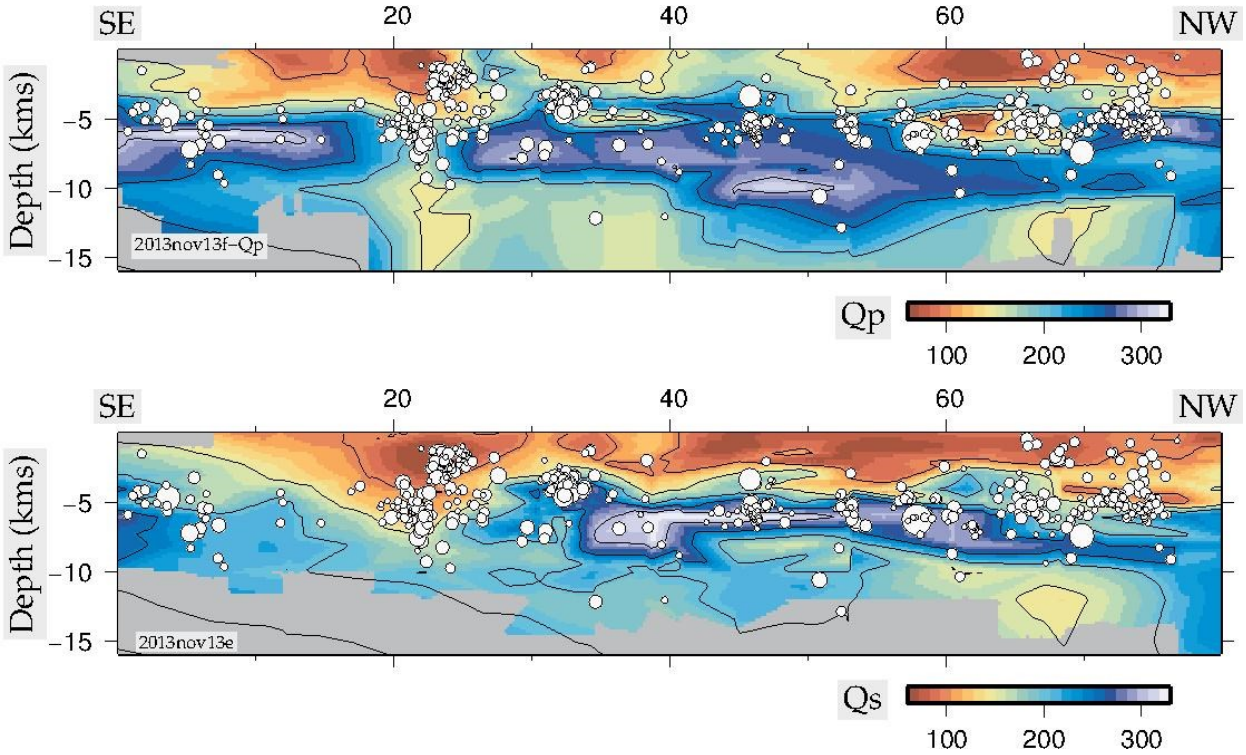

Figure 5: SE-NW cross-section of (top) Qp, and (bottom) Qs, along the profile shown in Figure 1a. Areas that are not well constrained are masked, based on the derivative-weight-sum (DWS). Wairakei seismicity is projected onto this cross-section at X=20-25 km and Waitapu-Waimangu seismicity at X=65-75 km.

4. CONCLUSION

We investigate seismic properties (Vp, Vs, Q) in the central Taupo Volcanic Zone, with a focus on the 3-to-8 km depth range. Intensive passive-seismic array measurements were carried out across the region by GNS Science between 2009 and 2011, using a 38-station broadband and short-period seismometer array. We use that data in this study to resolve new 3D seismic property volumes for the region north of Lake Taupo and south of Reporoa caldera.

Results from the seismic inversions highlight the variability of seismic properties in the mid-crust beneath the region, at a variety of scales, both spatially and in depth. The new seismic velocity volumes allows us to relocate all seismicity in the central Taupo Volcanic Zone, which will assist us in the future to define the lateral and depth variation of the seismic-aseismic transition beneath the region.

5. ACKNOWLEDGEMENTS

We thank Craig Miller, Nick Horspool, GNS Science Wairakei technicians, and GNS Science Wairakei staff for their logistical support in the seismic data collection during 2004-2005, and 2009-2011. National seismometer network data were provided by GeoNet (www.geonet.org.nz), which is sponsored by the New Zealand Government through its agencies Earthquake Commission

(EQC), GNS Science, and Land Information New Zealand (LINZ). We used GMT (Wessel & Smith, 1998) and ObsPy (Beyreuther et al., 2010) for figures. We thank Haijiang Zhang for use of his software. This research was carried out under the GNS Science CORE geothermal programme, funded by the New Zealand government.

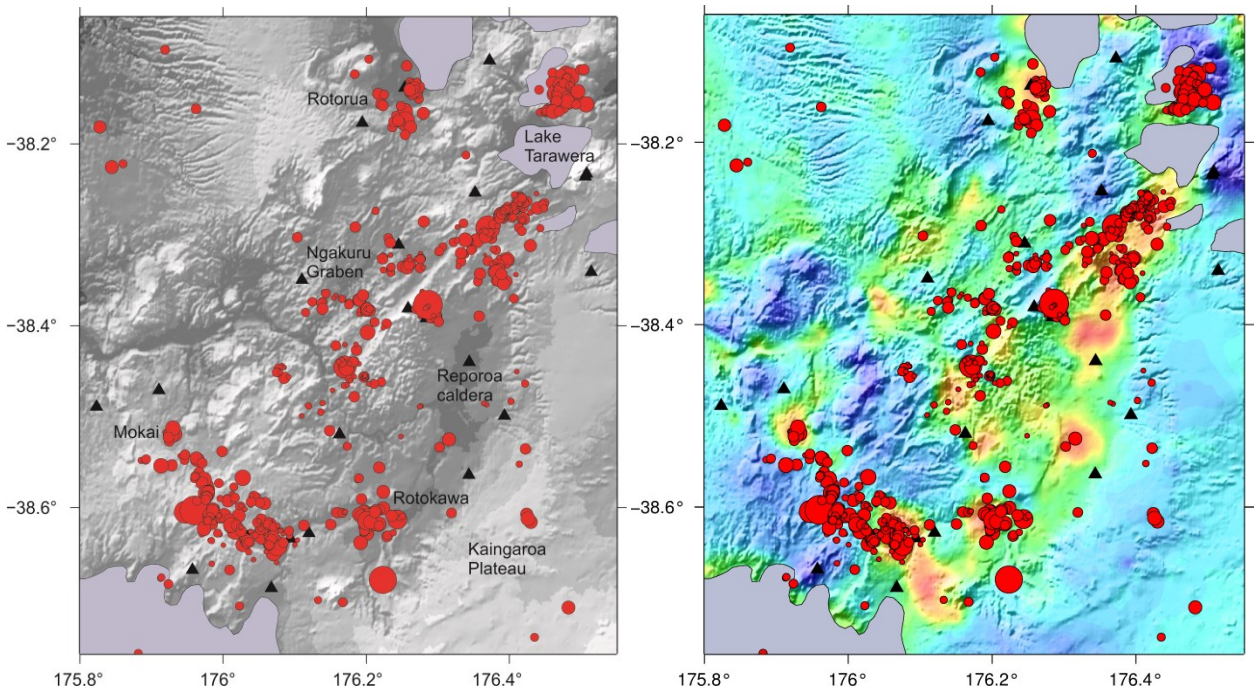

Figure 6 (left): Seismicity – relocated, for 1995-2013, for all well-constrained events shallower than 50 km depth. distributed across Ngakuru graben and known active faults ; Waimangu and Lake Tarawera – tightly clustered ; Note that many events recorded by GeoNet e.g. in late 1990s and early 2000s were not well constrained in location, and do not appear on this figure. Seismicity is associated with west-Wairakei geothermal field, Rotokawa geothermal field, and Mokai field. Other clusters of seismicity are evident near Waiotapu, and north-west of Waimangu. Figure 6b (right): Seismicity overlayen on resistivity, from Bibby et al. (1995).

REFERENCES

Adams, C.J., Mortimer, N., Campbell, H.J., Griffin, W.L., 2009. Age and isotropic characterization of metasedimentary rocks from the Torlesse SuperGroup and Waipapa Group in the central North Island, New Zealand. *New Zealand Journal of Geology and Geophysics*, 52:2, 149-170.

Bannister, S, Bourguignon, S., Sherburn, S., and T. Bertrand. 2013. Seismc imaging of the Central Taupo Volcanic Zone using double-difference tomography. *New Zealand Geothermal Workshop 2013 Proceedings*, 17-20 November 2013, Rotorua, New Zealand.

Bedrosian, P.A., Maercklin,N., Weckmann, U., Bartov, Y., Ryberg, T., and O.Ritter, (2007). Lithology-derived structure classification from the joint interpretation of megnetotelluric and seismic models. *Geophys. J. Int.*, 170(2), 737-748.

Bennington, N., Thurber, C., and S. Roecker. Three-dimensional attenuation structure around the SAFOD site, Parkfield, California (2008). Bull. *Seismological. Soc. Am.*, 98, 2934-2947. Doi:10.1785/0120080175.

Bertrand, E.A.; Caldwell, T.G.; Hill, G.J.; Wallin, E.L.; Bennie, S.L.; Cozens, N.; Onacha, S.A.; Ryan, G.A.; Walter, C.; Zaino, A.; Wameyo, P. 2012b, Magnetotelluric imaging of upper-crustal convection plumes beneath the Taupo Volcanic Zone, New Zealand. Geophysical Research Letters, 39(2): L02304, doi:10.1029/2011GL050177 (6 p.)

Bertrand, E.A., Caldwell, T.G., et al., 2012a, Deep geothermal exploration in the Taupo Volcanic Zone with an array of magnetotelluric and passive-seismic data. *New Zealand Geothermal Workshop Proceedings*, 2012.

Bertrand, E.A., Caldwell, T.G., Hill, G.J., Bennie, S.L., Soungkono, S., 2013. Magnetotelluric imaging of the Ohaaki geothermal system, New Zealand: implications for locating basement permeability. Journal of Volcanology and Geothermal Research, 268: 36-45.

Beyreuther, M., Barsch, R., Krischer, L., Megies, T., Behr, Y., and J.Wassermann, (2010). ObsPy: A python toolbox for seismology, *Seismological Research Letters*, doi::10.1785/gssrl.81.3.530.

Bibby, H.M., Caldwell, T.G., Davey, F.J., Webb, T.H. (1995), Geophysical evidence on the structure of the Taupo Volcanic Zone and its Hydrothermal Circulation. *Journal of Volcanology and Geothermal Research*, 68, 29-58.

Bignall, G., Hotter and Deeper: New Zealand's research programme to harness its deep geothermal resources. *Proceedings World Geothermal Congress*, 2010, Bali, Indonesia, 25-29 April 2010.

Bryan, C.J., Sherburn, S., Bibby, H.M., Bannister, S., Hurst, A.W., 1999. Shallow seismicity of the central Volcanic Zone, New Zealand: its distribution and nature. *New Zealand Journal of Geology and Geophysics*, 42(4): 533-542.

Eberhart-Phillips, D., Reyners, M., Chadwick, M., and Stuart, G., 2008. Three-dimensional attenuation structure of the Hikurangi subduction zone in the central North Island, New Zealand, *Geophys.J.Int*., 174, 418-434.

Eberhart-Phillips, D., Reyners, M.E., Bannister, S., Chadwick, M.P, Ellis, S.M., 2010. Establishing a versatile 3-D seismic velocity model for New Zealand. *Seismological research letters*, 81(6):992-1000. doi: 10.1785/gssrl.81.6.992.

Eberhart-Phillips, D., S. Bannister and S. Ellis, 2014. Imaging P and S attenuation in the termination region of the Hikurangi subduction zone, New Zealand. *Geophysical Journal International*, (2014), doi:10.1093/gji/ggu151.

Fontaine, F.R., Benoit, I., and N.S.Bagdassarov, 2005. Temperature dependence of shear wave attenuation in partially molten gabbronorite at seismic frequencies. *Geophysical Journal International*, 163, 1025-1038.

Harrison, A.J., and R.S.White (2006). Lithospheric structure of an active backarc basin: the Taupo Volcanic Zone, New Zealand. *Geophysical Journal International*, 167, 969-990, doi:10.1111/j.1365-246X.2006.03166.x

Heise, W., Caldwell, T.G., Bibby, H.M., and S.L.Bennie, 2010. Three-dimensional electrical resistivity image of magma beneath an active continental rift, Taupo Volcanic Zone, New Zealand. *Geophysical Research Letters*, 37, L10301, doi:10.1029/2010GL043110.

Henrys, S., Bannister, S., Pecher, I.A., Davey, F.J., Stern, T., Stratford, W., White, R., Harrison, A.J., Nishimura, Y., Yamada, A., 2003. New Zealand North Island GeopHysical Transect (NIGHT): field acquisition report. Lower Hutt: Institute of Geological & Nuclear Sciences Limited. *Institute of Geological & Nuclear Sciences science report* 2003/19. 49 p.

Paige, C., and M., Saunders (1982). LSQR: An algorithm for sparse linear equations and least squares problems, *Trans. Math. Software*, 8, 43-71.

Peacock, S., McCann, C., Sothcott, J., and Astin, T.R., 1994. Experimental measurements of seismic attenuation in microfractured sedimentary rock, *Geophysics*, 59, 1342-1351.

Petersen, T., Gledhill, K., Chadwick, M., Gale, N.H., and J.Ristau (2011). The New Zealand national seismograph network. *Seismological research letters*, 81, doi: 10.1785/gssrl.82.1.9

Reyners, M.E., Eberhart-Phillips, D., Stuart, G., Nishimuria, Y., 2006. Imaging subduction from the trench to 300 km depth beneath the central North Island, New Zealand, with Vp and Vp/Vs. *Geophysical Journal International* 165(2): 565-583.

Sherburn, S., Bannister, S., Bibby, H.M., 2003. Seismic velocity structure of the central Volcanic Zone, New Zealand, from local earthquake tomography. *Journal of Volcanology and Geothermal Research*, 122(1-2): 69-88.

Thurber, C.H. (1993). Local earthquake tomography: Velocities and Vp/Vs – Theory, in *Seismic Tomography: Theory and Practice*, edited by H. Iyer and K. Hirahara, pp. 563-580, CRC Press, Boca Raton, Fla.

Thurber, C.H. and Eberhart-Phillips, D., 1999. Local earthquake tomography with flexible gridding. *Comput. Geosci.,* 25, 809-818, doi:10.1016/S0098-3004(99)00007-2.

Waldhauser, F., and W.L. Ellsworth (2000). A double-difference earthquake location algorithm,: Method and application to the northern Hayward fault, California. *Bull.Seismological Society Am.*, 90, 1353-1368.

Waldhauser, F., (2001). *hypoDD* – A program to compute double-difference hypocenter locations (hypoDD version 1.0-03/2001). *USGS Open File report 01-11.*

Wessel, P., and W.H.F. Smith (1998). New, improved, version of the Generic Mapping Tools released, *EOS Trans.AGU*, 79, 579, 1998.

Wilson, C.J.N., Houghton, B.F., McWilliams, M.O., Lanphere, M.A., Weaver,S.D., and R.M.Briggs, 1995. Volcanic and structural evolution of Taupo Volcanic Zone, a review. *Journal of Volcanology and Geothermal Research*, 68, 1-28.

Wilson, C., Blake, S., Charlier, B.L.A., and A.N.Sutton, (2006). The 26.5 kz Oruanui Eruption, Taupo Volcano, New Zealand: Development, characteristics and evacuation of a large rhyolitic magma body, *Journal of Petrology*, 47, 35-69.

Zhang, Haijiang, & Thurber, C. (2006). Development and Applications of Double-difference Seismic Tomography. *Pure and Applied Geophysics*, 163(2-3), 373–403. doi:10.1007/s00024-005-0021-y

Zhang, Haijiang, Thurber, C., & Bedrosian, P. Joint inversion for Vp, Vs, and Vp/Vs at SAFOD, Parkfield, California. *Geochemistry Geophysics Geosystems*, 10(11), (2009) 1–17. doi:10.1029/2009GC002709

Zhang, Haijiang, & Thurber, C. H. (2003). Double-Difference Tomography: The Method and Its Application to the Hayward Fault, California. *Bulletin of the Seismological Society of America*, 93(5), 1875–1889. doi:10.1785/0120020190